Generic Case of Leap-Frog Algorithm for Optimal Knots Selection in Fitting Reduced Data

Ryszard Kozera[1,2][0000−0002−2907−8632], Lyle Noakes[2][0000−0001−9595−0735], and Artur Wiliński[1][0000−0002−3774−5909]

[1] Warsaw University of Life Sciences - SGGW, Institute of Information Technology Ul. Nowoursynowska 159, 02-776 Warsaw, Poland
{ryszard_kozera,artur_wilinski}@sggw.edu.pl
[2] The University of Western Australia, Faculty of Engineering and Mathematical Sciences, 35 Stirling Highway, Crawley, W.A. 6009 Perth, Australia
lyle.noakes@uwa.edu.au

Abstract. The problem of fitting multidimensional reduced data $\mathcal{M}_n$ is discussed here. The unknown interpolation knots $\mathcal{T}$ are replaced by optimal knots which minimize a highly non-linear multivariable function $\mathcal{J}_0$. The numerical scheme called *Leap-Frog Algorithm* is used to compute such optimal knots for $\mathcal{J}_0$ via the iterative procedure based in each step on single variable optimization of $\mathcal{J}_0^{(k,i)}$. The discussion on conditions enforcing unimodality of each $\mathcal{J}_0^{(k,i)}$ is also supplemented by illustrative examples both referring to the generic case of *Leap-Frog*. The latter forms a new insight on fitting reduced data and modelling interpolants of $\mathcal{M}_n$.

Keywords: Interpolation · Optimization · Curve modelling.

1 Introduction

In this work the problem of interpolating n points $\mathcal{M}_n = \{x_i\}_{i=0}^n$ in arbitrary Euclidean space $\mathbb{E}^m$ is addressed. The corresponding knots $\mathcal{T} = \{t_i\}_{i=0}^n$ are assumed to be unknown. The class of fitting functions (curves) $\mathcal{I}$ considered in this paper represents piecewise C^2 curves $\gamma : [0, T] \to \mathbb{E}^m$ satisfying $\gamma(t_i) = q_i$ and $\ddot{\gamma}(t_0) = \ddot{\gamma}(T) = \mathbf{0}$. It is also assumed that $\gamma \in \mathcal{I}$ is at least of class C^1 over $\mathcal{T}_{int} = \{t_i\}_{i=1}^{n-1}$ and extends to $C^2([t_i, t_{i+1}])$. Additionally, *the unknown internal knots* $\mathcal{T}_{int}$ are allowed to *vary* subject to $t_i < t_{i+1}$, for $i = 0, 1, \ldots, n-1$ (here $t_0 = 0$ and $t_n = T$). Such knots are called admissible and choosing them according to some adopted criterion permits *to control and model* the trajectory of γ. One of such criterion might focus on minimizing "average acceleration" of γ. In fact, for a given choice of fixed knots $\mathcal{T}$, the task of minimizing

$$\mathcal{J}_T(\gamma) = \sum_{i=0}^{n-1} \int_{t_i}^{t_{i+1}} \|\ddot{\gamma}(t)\|^2 dt \,, \tag{1}$$

(over $\mathcal{I}$) yields a unique optimal curve $\gamma_{opt} \in \mathcal{I}$ forming *a natural cubic spline* γ_{NS} - see [1] or [8]. Consequently, letting the internal knots $\mathcal{T}_{int}$ to change,

ICCS Camera Ready Version 2021
To cite this paper please use the final published version:
DOI: 10.1007/978-3-030-77970-2_26

minimizing $\mathcal{J}_T$ over $\mathcal{I}$ reduces into searching for an optimal natural spline γ_{NS} with $\mathcal{T}_{int}$ treated as free variables. Thus by [1], having recalled that γ_{NS} is uniquely determined by $\mathcal{T}$, minimizing $\mathcal{J}_T$ amounts to optimizing a highly non-linear function J_0 in $n-1$ variables $\mathcal{T}_{int}$ satisfying $t_i < t_{i+1}$ (see [3]). Due to the high non-linearity of J_0 the majority of numerical schemes applied to optimize J_0 lead to numerical difficulties (see e.g. [3]). Similarly, the analysis of critical points of J_0 forms a complicated task. To alleviate the latter, *a Leap-Frog* can be applied to deal with J_0 - see [2] or [3]. This scheme minimizes J_0 with iterative sequence of single variable overlapping optimizations of $J_0^{(k,i)}$ subject to $t_i < t_{i+1}$.

The novelty of this work refers to *the generic* case of *Leap-Frog* (recursively applied over each internal snapshots). The analysis establishing sufficient conditions for *unimodality* of $J_0^{(k,i)}$ is conducted here. Numerical tests and illustrative examples supplement the latter. The discussion covers first a special case of data (see Section 4) extended next to its perturbation (see Section 5 and Th. 1). More information on numerical performance of *Leap-Frog* and comparison tests with two standard numerical optimization schemes can be found in [2], [3] or recently published [6]. Some applications of *Leap-Frog* optimization scheme used also as a modelling and simulation tool are discussed in [9], [10] or [11].

2 Preliminaries

Recall (see [1]) that *a cubic spline interpolant* $\gamma_{\mathcal{T}}^{C_i} = \gamma_{\mathcal{T}}^{C}|_{[t_i,t_{i+1}]}$, for a given admissible knots $\mathcal{T} = (t_0, t_1, \ldots, t_{n-1}, t_n)$ is defined as $\gamma_{\mathcal{T}}^{C_i}(t) = c_{1,i} + c_{2,i}(t - t_i) + c_{3,i}(t-t_i)^2 + c_{4,i}(t-t_i)^3$, (for $t \in [t_i, t_{i+2}]$) to satisfy (for $i = 0, 1, 2, \ldots, n-1$; $c_{j,i} \in \mathbb{R}^m$, where $j = 1, 2, 3, 4$) $\gamma_{\mathcal{T}}^{C_i}(t_{i+k}) = x_{i+k}$ and $\dot{\gamma}_{\mathcal{T}}^{C_i}(t_{i+k}) = v_{i+k}$, for $k = 0, 1$ with the velocities $v_0, v_1, \ldots, v_{n-1}, v_n \in \mathbb{R}^m$ assumed to be temporarily free parameters (*if unknown*). The coefficients $c_{j,i}$ read (with $\Delta t_i = t_{i+1} - t_i$):

$$c_{1,i} = x_i, \qquad c_{2,i} = v_i\ ,$$
$$c_{4,i} = \frac{v_i + v_{i+1} - 2\frac{x_{i+1}-x_i}{\Delta t_i}}{(\Delta t_i)^2}\ , \qquad c_{3,i} = \frac{\frac{(x_{i+1}-x_i)}{\Delta t_i} - v_i}{\Delta t_i} - c_{4,i}\Delta t_i\ . \tag{2}$$

The latter follows from Newton's divided differences formula (see e.g. [1, Chap.1]). Adding $n-1$ constraints $\ddot{\gamma}_{\mathcal{T}}^{C_{i-1}}(t_i) = \ddot{\gamma}_{\mathcal{T}}^{C_i}(t_i)$ for continuity of $\ddot{\gamma}_{\mathcal{T}}^{C}$ at $x_1, \ldots, x_{n-1}$ (with $i = 1, 2, \ldots, n-1$) leads by (2) (for $\gamma_{\mathcal{T}}^{C_i}$) to the m tridiagonal linear systems (strictly diagonally dominant) of $n-1$ equations in $n+1$ vector unknowns representing velocities at $\mathcal{M}$ i.e. $v_0, v_1, v_2, \ldots, v_{n-1}, v_n \in \mathbb{R}^m$:

$$v_{i-1}\Delta t_i + 2v_i(\Delta t_{i-1} + \Delta t_i) + v_{i+1}\Delta t_{i-1} = b_i\ ,$$
$$b_i = 3(\Delta t_i \frac{x_i - x_{i-1}}{\Delta t_{i-1}} + \Delta t_{i-1}\frac{x_{i+1} - x_i}{\Delta t_i})\ . \tag{3}$$

(i) Both v_0 and v_n (*if unknown*) can be e.g. calculated from $a_0 = \ddot{\gamma}_{\mathcal{T}}^{C}(0) = a_n = \ddot{\gamma}_{\mathcal{T}}^{C}(T_c) = \mathbf{0}$ combined with (2) (this yields *a natural cubic spline interpolant* $\gamma_{\mathcal{T}}^{NS}$ - a special $\gamma_{\mathcal{T}}^{C}$) which supplements (3) with two missing vector linear equations:

$$2v_0 + v_1 = 3\frac{x_1 - x_0}{\Delta t_0}\ , \quad v_{n-1} + 2v_n = 3\frac{x_n - x_{n-1}}{\Delta t_{n-1}}\ . \tag{4}$$

ICCS Camera Ready Version 2021
To cite this paper please use the final published version:
DOI: 10.1007/978-3-030-77970-2_26

The resulting m linear systems, each of size $n+1\times n+1$, (based on (3) and (4)) as strictly row diagonally dominant result in one vector solution $v_0, v_1, \ldots, v_{n-1}, v_n$ (solved e.g. by Gauss elimination without pivoting - see [1, Chap. 4]), which when fed into (2) determines explicitly *a natural cubic spline* $\gamma_{\mathcal{T}}^{NS}$ (with fixed $\mathcal{T}$). A similar approach follows for arbitrary a_0 and a_n.
(ii) If both v_0 and v_n are given then the so-called *complete spline* $\gamma_{\mathcal{T}}^{CS}$ can be found with $v_1, \ldots v_{n-1}$ determined solely by (3).
(iii) If one of v_0 or v_n is unknown it can be compensated by setting the respective terminal acceleration e.g. to $\mathbf{0}$. The above scheme relies on solving (3) with one equation from (4). Such splines are denoted here by $\gamma_{\mathcal{T}}^{v_n}$ or $\gamma_{\mathcal{T}}^{v_0}$. Two *non-generic* cases of *Leap-Frog* optimizations deal with the latter - omitted in this paper.

By (1) $\mathcal{J}_T(\gamma_{\mathcal{T}}^{NS}) = 4\sum_{i=0}^{n-1}(\|c_{3,i}\|^2\Delta t_i + 3\|c_{4,i}\|^2(\Delta t_i)^3 + 3\langle c_{3,i}|c_{4,i}\rangle(\Delta t_i)^2)$, which ultimately reformulates into (see [2]):

$$\mathcal{J}_T(\gamma_{\mathcal{T}}^{NS}) = 4\sum_{i=0}^{n-1}\Big(\frac{-1}{(\Delta t_i)^3}(-3\|x_{i+1}-x_i\|^2 + 3\langle v_i + v_{i+1}|x_{i+1}-x_i\rangle\Delta t_i \\ -(\|v_i\|^2 + \|v_{i+1}\|^2 + \langle v_i|v_{i+1}\rangle)(\Delta t_i)^2\Big)\,. \tag{5}$$

As mentioned before for fixed knots $\mathcal{T}$, the natural spline $\gamma_{\mathcal{T}}^{NS}$ minimizes (1) (see [1]). Thus upon relaxing the internal knots $\mathcal{T}_{int}$ the original infinite dimensional optimization (1) reduces itself into finding the corresponding *optimal knots* $(t_1^{opt}, t_2^{opt}, \ldots, t_{n-1}^{opt})$ for (5) (viewed from now on as a multivariable function $J_0(t_1, t_2, \ldots, t_{n-1})$) subject to $t_0 = 0 < t_1^{opt} < t_2^{opt} < \cdots < t_{n-1}^{opt} < t_n = T$. Such reformulated non-linear optimization task (5) transformed into minimizing $J_0(\mathcal{T}_{int})$ (here $t_0 = 0$ and $t_n = T$) forms a difficult task for critical points examination as well as for the numerical computations. The analysis addressing the non-linearity of J_0 and comparisons between different numerical methods used to optimize J_0 are discussed in [2], [3] or [6]. One of the computationally feasible schemes handling (5) turns out to be *a Leap-Frog* (for its $2D$ analogue for image noise removal see also [11] or in other contexts see e.g. [9] or [10]). For optimizing J_0 this scheme is based on the sequence of single variable iterative optimization which in k-th iteration minimizes:

$$J_0^{(k,i)}(s) = \int_{t_{i-1}^k}^{t_{i+1}^{k-1}} \|\ddot{\gamma}_{k,i}^{CS}(s)\|^2 ds \tag{6}$$

over $I_i^{k-1} = [t_{i-1}^k, t_{i+1}^{k-1}]$. Here t_i is set to be a free variable s_i. The complete spline $\gamma_{k,i}^{CS} : I_i^{k-1} \to \mathbb{E}^m$ is determined by $\{t_{i-1}^k, s, t_{i+1}^{k-1}\}$, both velocities $\{v_{i-1}^k, v_{i+1}^{k-1}\}$ and the interpolation points $\{x_{i-1}, x_i, x_{i+1}\}$. Once s_i^{opt} is found one updates t_i^{k-1} with $t_i^k = s_i^{opt}$ and v_i^{k-1} with the $v_i^k = \dot{\gamma}_{k,i}^{CS}(s_i^{opt})$. Next we pass to the shifted overlapped sub-interval $I_{i+1}^k = [t_i^k, t_{i+2}^{k-1}]$ and repeat the previous step of updating t_{i+1}^{k-1}. Note that both cases $[0, t_2^{k-1}]$ and $[t_{n-2}^{k-1}, T]$ rely on splines discussed in *(iii)*, where the vanishing acceleration replaces one of the velocities v_0^{k-1} or v_n^{k-1}. Once t_{n-1}^{k-1} is changed over the last sub-interval $I_{n-1}^{k-1} = [t_{n-2}^k, T]$ the k-th iteration

ICCS Camera Ready Version 2021
To cite this paper please use the final published version:
DOI: 10.1007/978-3-030-77970-2_26

is terminated and the next local optimization over $I_1^k = [0, t_2^k]$ represents the beginning of the $(k+1)$-st iteration of *Leap-Frog Algorithm*. The initialization of $\mathcal{T}_{int}$ for *Leap-Frog* can follow normalized *cumulative chord parameterization* (see e.g. [8]) which sets $t_0^0 = 0, t_1^0, \ldots, t_{n-1}^k, t_n^0 = T$ according to $t_0^0 = 0$ and $t_{i+1}^0 = \|x_{i+1} - x_i\| \frac{T}{\hat{T}} + t_i^0$, for $i = 0, 1, \ldots, n-1$ and $\hat{T} = \sum_{i=0}^{n-1} \|x_{i+1} - x_i\|$.

3 Generic Middle Case: Initial and Last Velocities Given

Assume that for internal points $x_i, x_{i+1}, x_{i+2} \in \mathbb{E}^m$ (for $i = 1, 2, \ldots, n-3$ and $n > 3$) the interpolation knots t_i and t_{i+2} with the velocities $v_i, v_{i+2} \in \mathbb{R}^m$ are somehow given (e.g. by previous *Leap-Frog* iteration outlined in Section 2). We construct now a C^2 piecewise cubic (a complete spline - see Section 2), depending on varying $t_{i+1} \in (t_i, t_{i+2})$ (temporarily free variable). The curve $\gamma_i^c : [t_i, t_{i+2}] \to \mathbb{E}^m$ (i.e. a cubic on each $[t_i, t_{i+1}]$ and $[t_{i+1}, t_{i+2}]$) satisfies:

$$\gamma_i^c(t_{i+j}) = x_{i+j} \ , \quad j = 0, 1, 2 \ ; \quad \dot{\gamma}_i^c(t_{i+j}) = v_{i+j} \ , \quad j = 0, 2 \ . \tag{7}$$

Letting $\phi_i : [t_i, t_{i+2}] \to [0, 1]$, $\phi_i(t) = (t - t_i)(t_{i+2} - t_i)^{-1} = s$ the curve $\tilde{\gamma}_i^c : [0, 1] \to \mathbb{E}^m$ (with $\tilde{\gamma}_i^c = \gamma_i^c \circ \phi_i^{-1}$) by (7) satisfies, for $0 < s_{i+1} = \phi_i(t_{i+1}) < 1$:

$$\tilde{\gamma}_i^c(0) = x_i \ , \quad \tilde{\gamma}_i^c(s_{i+1}) = x_{i+1} \ , \quad \tilde{\gamma}_i^c(1) = x_{i+2} \ , \tag{8}$$

with the adjusted initial and the last velocities $\tilde{v}_i, \tilde{v}_{i+2} \in \mathbb{R}^m$ fulfilling:

$$\tilde{v}_i = \tilde{\gamma}_i^{c'}(0) = (t_{i+2} - t_i) v_i \ , \quad \tilde{v}_{i+2} = \tilde{\gamma}_i^{c'}(1) = (t_{i+2} - t_i) v_{i+2} \ . \tag{9}$$

To reformulate $\tilde{\mathcal{E}}_i$ define two cubics $\tilde{\gamma}_i^{lc}, \tilde{\gamma}_i^{rc}$ satisfying (with $s_{i+1} \in (0, 1)$) $\tilde{\gamma}_i^c = \tilde{\gamma}_i^{lc}$ (over $[0, s_{i+1}]$) and $\tilde{\gamma}_i^c = \tilde{\gamma}_i^{rc}$ (over $[s_{i+1}, 1]$) with $c_{ij}, d_{ij} \in \mathbb{E}^m$:

$$\begin{aligned} \tilde{\gamma}_i^{lc}(s) &= c_{i0} + c_{i1}(s - s_{i+1}) + c_{i2}(s - s_{i+1})^2 + c_{i3}(s - s_{i+1})^3 \ , \\ \tilde{\gamma}_i^{rc}(s) &= d_{i0} + d_{i1}(s - s_{i+1}) + d_{i2}(s - s_{i+1})^2 + d_{i3}(s - s_{i+1})^3 \ . \end{aligned} \tag{10}$$

Since $\tilde{\gamma}_i^c$ is a complete spline the following constraints hold:

$$\tilde{\gamma}_i^{lc}(0) = x_i \ , \quad \tilde{\gamma}_i^{lc}(s_{i+1}) = \tilde{\gamma}_i^{rc}(s_{i+1}) = x_{i+1} \ , \quad \tilde{\gamma}_i^{rc}(1) = x_{i+2} \ , \tag{11}$$

$$\tilde{\gamma}_i^{lc'}(0) = \tilde{v}_i \ , \qquad \tilde{\gamma}_i^{rc'}(1) = \tilde{v}_{i+2} \ , \tag{12}$$

together with two C^1 and C^2 smoothness constraints at $s = s_{i+1}$:

$$\tilde{\gamma}_i^{lc'}(s_{i+1}) = \tilde{\gamma}_i^{rc'}(s_{i+1}) \ , \qquad \tilde{\gamma}_i^{lc''}(s_{i+1}) = \tilde{\gamma}_i^{rc''}(s_{i+1}) \ . \tag{13}$$

As derivative is invariant, upon shifting the coordinates origin in $\mathbb{E}^m$ to x_{i+1} we have for $\tilde{x}_{i+1} = \mathbf{0}$, $\tilde{x}_i = x_i - x_{i+1}$ and $\tilde{x}_{i+2} = x_{i+2} - x_{i+1}$ (by (11)):

$$\tilde{\gamma}_i^{lc}(0) = \tilde{x}_i \ , \quad \tilde{\gamma}_i^{lc}(s_{i+1}) = \tilde{\gamma}_i^{rc}(s_{i+1}) = \mathbf{0} \ , \quad \tilde{\gamma}_i^{rc}(1) = \tilde{x}_{i+2} \ . \tag{14}$$

Both (10) and $x_{i+1} = \mathbf{0}$ yield $c_{i0} = d_{i0} = \mathbf{0}$. Next (13) with $\tilde{\gamma}_i^{lc'}(s) = c_{i1} + 2c_{i2}(s - s_{i+1}) + 3c_{i3}(s - s_{i+1})^2$, $\tilde{\gamma}_i^{rc'}(s) = d_{i1} + 2d_{i2}(s - s_{i+1}) + 3d_{i3}(s - s_{i+1})^2$,

ICCS Camera Ready Version 2021
To cite this paper please use the final published version:
DOI: 10.1007/978-3-030-77970-2_26

$\tilde{\gamma}_i^{lc''}(s) = 2c_{i2} + 6c_{i3}(s - s_{i+1})$ and $\tilde{\gamma}_i^{lr''}(s) = 2d_{i2} + 6d_{i3}(s - s_{i+1})$, leads to $c_{i1} = d_{i1}$ and $c_{i2} = d_{i2}$. Hence one obtains:

$$\begin{aligned}\tilde{\gamma}_i^{lc}(s) &= c_{i1}(s - s_{i+1}) + c_{i2}(s - s_{i+1})^2 + c_{i3}(s - s_{i+1})^3 \,, \\ \tilde{\gamma}_i^{rc}(s) &= c_{i1}(s - s_{i+1}) + c_{i2}(s - s_{i+1})^2 + d_{i3}(s - s_{i+1})^3 \,. \end{aligned} \tag{15}$$

The unknown vectors $c_{i1}, c_{i2}, c_{i3}, d_{i3}$ in (15) follow from four linear vector equations obtained from (12) and (14) (i.e. with data $\tilde{\mathcal{M}}_i = \{\tilde{x}_i, \tilde{x}_{i+2}, \tilde{v}_i, \tilde{v}_{i+2}\}$):

$$\begin{aligned}\tilde{x}_i &= -c_{i1}s_{i+1} + c_{i2}s_{i+1}^2 - c_{i3}s_{i+1}^3 \,, \\ \tilde{x}_{i+2} &= c_{i1}(1 - s_{i+1}) + c_{i2}(1 - s_{i+1})^2 + d_{i3}(1 - s_{i+1})^3 \,, \\ \tilde{v}_i &= c_{i1} - 2c_{i2}s_{i+1} + 3c_{i3}s_{i+1}^2 \,, \\ \tilde{v}_{i+2} &= c_{i1} + 2c_{i2}(1 - s_{i+1}) + 3d_{i3}(1 - s_{i+1})^2 \,. \end{aligned} \tag{16}$$

Upon invoking the *Mathematica* function *Solve* to handle (16) one arrives at:

$$\begin{aligned}c_{i1} &= -\frac{-s_{i+1}\tilde{v}_i + 2s_{i+1}^2\tilde{v}_i - s_{i+1}^3\tilde{v}_i - s_{i+1}^2\tilde{v}_{i+2} + s_{i+1}^3\tilde{v}_{i+2} - 3\tilde{x}_i + 6s_{i+1}\tilde{x}_i}{2(s_{i+1} - 1)s_{i+1}} \\ &\quad -\frac{-3s_{i+1}^2\tilde{x}_i + 3s_{i+1}^2\tilde{x}_{i+2}}{2(s_{i+1} - 1)s_{i+1}} \,, \\ c_{i2} &= -\frac{s_{i+1}\tilde{v}_i - s_{i+1}^2\tilde{v}_i - s_{i+1}\tilde{v}_{i+2} + s_{i+1}^2\tilde{v}_{i+2} + 3\tilde{x}_i - 3s_{i+1}\tilde{x}_i + 3s_{i+1}\tilde{x}_{i+2}}{(s_{i+1} - 1)s_{i+1}} \,, \\ c_{i3} &= -\frac{s_{i+1}(\tilde{v}_i + 2\tilde{x}_i) - s_{i+1}^3(\tilde{v}_i - \tilde{v}_{i+2}) - s_{i+1}^2(\tilde{v}_{i+2} + 3\tilde{x}_i - 3\tilde{x}_{i+2}) + \tilde{x}_i}{2(s_{i+1} - 1)s_{i+1}^3} \,, \\ d_{i3} &= -\frac{-s_{i+1}\tilde{v}_i + 2s_{i+1}^2\tilde{v}_i - s_{i+1}^3\tilde{v}_i + 2s_{i+1}\tilde{v}_{i+2} - 3s_{i+1}^2\tilde{v}_{i+2} + s_{i+1}^3\tilde{v}_{i+2} - 3\tilde{x}_i}{2(s_{i+1} - 1)^3 s_{i+1}} \\ &\quad -\frac{6s_{i+1}\tilde{x}_i - 3s_{i+1}^2\tilde{x}_i - 4s_{i+1}\tilde{x}_{i+2} + 3s_{i+1}^2\tilde{x}_{i+2}}{2(s_{i+1} - 1)^3 s_{i+1}} \,, \end{aligned} \tag{17}$$

which satisfy (as functions in s_{i+1}) the system (16). Next, since $\|\gamma_i^{lc''}(s)\|^2 = 4\|c_{i2}\|^2 + 24\langle c_{i2}|c_{i3}\rangle(s - s_{i+1}) + 36\|c_{i3}\|^2(s - s_{i+1})^2$ and $\|\gamma_i^{rc''}(s)\|^2 = 4\|c_{i2}\|^2 + 24\langle c_{i2}|d_{i3}\rangle(s - s_{i+1}) + 36\|d_{i3}\|^2(s - s_{i+1})^2$ the formula for $\tilde{\mathcal{E}}_i$ reads as

$$\tilde{\mathcal{E}}_i(s_{i+1}) = \int_0^{s_{i+1}} \|\gamma_i^{lc''}(s)\|^2 ds + \int_{s_{i+1}}^1 \|\gamma_i^{rc''}(s)\|^2 ds = I_1 + I_2,$$

where $I_1 = 4(\|c_{i2}\|^2 s_{i+1} - 3\langle c_{i2}|c_{i3}\rangle s_{i+1}^2 + 3\|c_{i3}\|^2 s_{i+1}^3)$ and $I_2 = 4(\|c_{i2}\|^2(1 - s_{i+1}) + 3\langle c_{i2}|d_{i3}\rangle(1 - s_{i+1})^2 + 3\|d_{i3}\|^2(1 - s_{i+1})^3)$. Combining the latter with (17) (upon applying *NIntegrate* and *FullSimplify* from *Mathematica Package*) yields:

ICCS Camera Ready Version 2021
To cite this paper please use the final published version:
DOI: 10.1007/978-3-030-77970-2_26

$$\tilde{\mathcal{E}}_i(s_{i+1}) =$$
$$\frac{1}{s_{i+1}^3(s_{i+1}-1)^3}(3\|\tilde{x}_i\|^2(s_{i+1}-1)^3(1+3s_{i+1})+s_{i+1}(-6\langle\tilde{v}_i|\tilde{x}_i\rangle$$
$$+s_{i+1}(\|\tilde{v}_{i+2}\|^2(s_{i+1}-4)(s_{i+1}-1)^2s_{i+1}+3\|\tilde{x}_{i+2}\|^2s_{i+1}(3s_{i+1}-4)$$
$$+\|\tilde{v}_i\|^2(s_{i+1}-1)^3(s_{i+1}+3)-2(s_{i+1}-1)^3s_{i+1}\langle\tilde{v}_i|\tilde{v}_{i+2}\rangle$$
$$+6(2+(s_{i+1}-2)s_{i+1}^2)\langle\tilde{v}_i|\tilde{x}_i\rangle-6(s_{i+1}-1)^2s_{i+1}\langle\tilde{v}_i|\tilde{x}_{i+2}\rangle-6(s_{i+1}-1)^3\langle\tilde{v}_{i+2}|\tilde{x}_i\rangle$$
$$+6(s_{i+1}-2)(s_{i+1}-1)s_{i+1}\langle\tilde{v}_{i+2}|\tilde{x}_{i+2}\rangle-18(s_{i+1}-1)^2\langle\tilde{x}_i|\tilde{x}_{i+2}\rangle))) \ . \tag{18}$$

Upon substituting for $\tilde{x}_{i+2}=x_{i+2}-x_{i+1}$ and $\tilde{x}_i=x_i-x_{i+1}$ one can reformulate (18) (and thus (19)) in terms of each data $x_i,x_{i+1},x_{i+2}\in\mathbb{E}^m$. *Mathematica* symbolic differentiation and *FullSimplify* function applied to $\tilde{\mathcal{E}}_i$ yields: $\tilde{\mathcal{E}}_i'(s_{i+1}) =$

$$\frac{-3}{(s_{i+1}-1)^4s_{i+1}^4}(3\|\tilde{x}_i\|^2(s_{i+1}-1)^4(1+2s_{i+1})+s_{i+1}(\|\tilde{v}_i\|^2(s_{i+1}-1)^4s_{i+1}$$
$$-\|\tilde{v}_{i+2}\|^2(s_{i+1}-1)^2s_{i+1}^3+3\|\tilde{x}_{i+2}\|^2s_{i+1}^3(2s_{i+1}-3)$$
$$+2(s_{i+1}-1)^4(2+s_{i+1})\langle\tilde{v}_i|\tilde{x}_i\rangle-2(s_{i+1}-1)^2s_{i+1}^3\langle\tilde{v}_i|\tilde{x}_{i+2}\rangle$$
$$-2(s_{i+1}-1)^4s_{i+1}\langle\tilde{v}_{i+2}|\tilde{x}_i\rangle+2(s_{i+1}-3)(s_{i+1}-1)s_{i+1}^3\langle\tilde{v}_{i+2}|\tilde{x}_{i+2}\rangle$$
$$-6(s_{i+1}-1)^2s_{i+1}(2s_{i+1}-1)\langle\tilde{x}_i|\tilde{x}_{i+2}\rangle)) \ . \tag{19}$$

By (19) $\tilde{\mathcal{E}}_i'(s_{i+1})=(-1/((s_{i+1}-1)^4s_{i+1}^4))N_i(s_{i+1})$, where $N_i(s_{i+1})$ is a polynomial of degree 6 (use here e.g. *Mathematica* functions *Factor* and *CoefficientList*) $N_i(s_{i+1})=b_0^i+b_1^is_{i+1}+b_2^is_{i+1}^2+b_3^is_{i+1}^3+b_4^is_{i+1}^4+b_5^is_{i+1}^5+b_6^is_{i+1}^6$, where

$$\frac{b_0^i}{3}=3\|\tilde{x}_i\|^2 \ , \qquad \frac{b_1^i}{3} \ = \ -6\|\tilde{x}_i\|^2+4\langle\tilde{v}_i|\tilde{x}_i\rangle \ ,$$
$$\frac{b_2^i}{3}=\|\tilde{v}_i\|^2-6\|\tilde{x}_i\|^2-14\langle\tilde{v}_i|\tilde{x}_i\rangle-2\langle\tilde{v}_{i+2}|\tilde{x}_i\rangle+6\langle\tilde{x}_i|\tilde{x}_{i+2}\rangle \ ,$$
$$\frac{b_3^i}{3}=-4\|\tilde{v}_i\|^2+24\|\tilde{x}_i\|^2+16\langle\tilde{v}_i|\tilde{x}_i\rangle+8\langle\tilde{v}_{i+2}|\tilde{x}_i\rangle-24\langle\tilde{x}_i|\tilde{x}_{i+2}\rangle \ ,$$
$$\frac{b_4^i}{3}=6\|\tilde{v}_i\|^2-\|\tilde{v}_{i+2}\|^2-21\|\tilde{x}_i\|^2-9\|\tilde{x}_{i+2}\|^2-4\langle\tilde{v}_i|\tilde{x}_i\rangle-2\langle\tilde{v}_i|\tilde{x}_{i+2}\rangle$$
$$-12\langle\tilde{v}_{i+2}|\tilde{x}_i\rangle+6\langle\tilde{v}_{i+2}|\tilde{x}_{i+2}\rangle+30\langle\tilde{x}_i|x_{i+2}\rangle \ ,$$
$$\frac{b_5^i}{3}=-4\|\tilde{v}_i\|^2+2\|\tilde{v}_{i+2}\|^2+6\|\tilde{x}_i\|^2+6\|\tilde{x}_{i+2}\|^2-4\langle\tilde{v}_i|\tilde{x}_i\rangle+4\langle\tilde{v}_i|\tilde{x}_{i+2}\rangle\rangle$$
$$+8\langle\tilde{v}_{i+2}|\tilde{x}_i\rangle-8\langle\tilde{v}_{i+2}|\tilde{x}_{i+2}\rangle-12\langle\tilde{x}_i|\tilde{x}_{i+2}\rangle \ ,$$
$$\frac{b_6^i}{3}=\|\tilde{v}_i\|^2-\|\tilde{v}_{i+2}\|^2+2\langle\tilde{v}_i|\tilde{x}_i\rangle-2\langle\tilde{v}_i|\tilde{x}_{i+2}\rangle-2\langle\tilde{v}_{i+2}|\tilde{x}_i\rangle+2\langle\tilde{v}_{i+2}|\tilde{x}_{i+2}\rangle \ .$$

In a search for a global optimum of $\tilde{\mathcal{E}}_i$, instead of using any optimization scheme relying on initial guess, one can apply *Mathematica Package Solve* which finds all roots (real and complex). Indeed upon computing the roots of $N_i(s_{i+1})$ one selects only these from $(0,1)$. Next we evaluate $\tilde{\mathcal{E}}_i$ on each critical point $s_{i+1}^{crit}\in(0,1)$ and choose s_{i+1}^{crit} with minimal energy as optimal. This feature is particularly useful in implementation of Leap-Frog as opposed to the optimization of the initial energy (5) depending on $n-1$ unknown knots.

ICCS Camera Ready Version 2021
To cite this paper please use the final published version:
DOI: 10.1007/978-3-030-77970-2_26

4 Special Conditions for Leap-Frog Generic Case

Assume $\tilde{x}_i, \tilde{x}_{i+1}, \tilde{x}_{i+2} \in \mathbb{E}^m$ with $\tilde{v}_i, \tilde{v}_{i+2} \in \mathbb{R}^m$ satisfy now the extra constraints:

$$\tilde{v}_i = \tilde{v}_{i+2} \ , \qquad \tilde{x}_{i+2} - \tilde{x}_i = \tilde{v}_i = \tilde{v}_{i+2} \ . \tag{20}$$

By (20) we get $\|\tilde{v}_{i+2}\|^2 = \|\tilde{v}_i\|^2 = \langle \tilde{v}_i | \tilde{v}_{i+2} \rangle = \|\tilde{x}_{i+2}\|^2 + \|\tilde{x}_i\|^2 - 2\langle \tilde{x}_i | \tilde{x}_{i+2} \rangle$, $\langle \tilde{x}_i | \tilde{v}_i \rangle = \langle \tilde{x}_i | \tilde{v}_{i+2} \rangle = \langle \tilde{x}_i | \tilde{x}_{i+2} \rangle - \|\tilde{x}_i\|^2$ and $\langle \tilde{x}_{i+2} | \tilde{v}_i \rangle = \langle \tilde{x}_{i+2} | \tilde{v}_{i+2} \rangle = \|\tilde{x}_{i+2}\|^2 - \langle \tilde{x}_i | \tilde{x}_{i+2} \rangle$. Substituting the above into (19) (or into $\tilde{\mathcal{E}}_i^c$) yields $\tilde{\mathcal{E}}_i^c(s_{i+1}) =$

$$-\frac{3(\|\tilde{x}_i\|^2(s_{i+1}-1)^2 + s_{i+1}(\|\tilde{x}_{i+2}\|^2 s_{i+1} - 2(s_{i+1}-1)\langle \tilde{x}_i | \tilde{x}_{i+2} \rangle))}{(s_{i+1}-1)^3 s_{i+1}^3} \tag{21}$$

and hence $\tilde{\mathcal{E}}_i^{c'}(s_{i+1}) =$

$$\begin{aligned} &\frac{3}{(s_{i+1}-1)^4 s_{i+1}^4}(\|\tilde{x}_i\|^2(s_{i+1}-1)^2(4s_{i+1}-3) \\ &+s_{i+1}(\|\tilde{x}_{i+2}\|^2 s_{i+1}(4s_{i+1}-1) - 4(1-3s_{i+1}+2s_{i+1}^2)\langle \tilde{x}_i | \tilde{x}_{i+2} \rangle)) \ . \end{aligned} \tag{22}$$

The numerator of (22) forms now a polynomial of degree 3 (instead of degree 6 as in (19)) $N_i^c(s_{i+1}) = b_0^{i_c} + b_1^{i_c} s_{i+1} + b_2^{i_c} s_{i+1}^2 + b_3^{i_c} s_{i+1}^3$, where:

$$\begin{aligned} &\frac{b_0^{i_c}}{3} = -3\|\tilde{x}_i\|^2 < 0 \ , \qquad \frac{b_1^{i_c}}{3} \ = \ 2(5\|\tilde{x}_i\|^2 - 2\langle \tilde{x}_i | \tilde{x}_{i+2} \rangle) \ , \\ &\frac{b_2^{i_c}}{3} = -11\|\tilde{x}_i\|^2 - \|\tilde{x}_{i+2}\|^2 + 12\langle \tilde{x}_i | \tilde{x}_{i+2} \rangle = 5(\|\tilde{x}_{i+2}\|^2 - \|\tilde{x}_i\|^2) - 6\|\tilde{x}_{i+2} - \tilde{x}_i\|^2 \ , \\ &\frac{b_3^{i_c}}{3} = 4\|\tilde{x}_i\|^2 + 4\|\tilde{x}_{i+2}\|^2 - 8\langle \tilde{x}_i | \tilde{x}_{i+2} \rangle = 4\|\tilde{x}_{i+2} - \tilde{x}_i\|^2 \geq 0 \ . \end{aligned}$$

For $\tilde{\mathcal{E}}_i^c$ to be unimodal over $(0,1)$ one needs $N_i^c(s_{i+1})$ with a single root in $(0,1)$. *(i)* Note that if $\tilde{x}_{i+2} = \tilde{x}_i$ then $N_i^c(s_{i+1}) = -9\|\tilde{x}_i\|^2 + 18 s_{i+1}\|\tilde{x}_i\|^2$ has exactly one root $\hat{s}_{i+1} = 1/2 \in (0,1)$. By (20) we have $\tilde{v}_{i+2} = \tilde{v}_i = \mathbf{0}$.
(ii) We assume now that $\tilde{x}_{i+2} \neq \tilde{x}_i$ then $N_i^c(s_{i+1})$ becomes *a cubic*. We find now the conditions for which N_i^c has exactly one root over $(0,1)$. For the latter as $N_i^c(0) = -9\|\tilde{x}_i\|^2 < 0$ and $N_i^c(1) = 9\|\tilde{x}_{i+2}\|^2 > 0$ by Intermediate Value Th. it suffices to show that either $N_i^{c'}(s_{i+1}) = c_0^{i_c} + c_1^{i_c} s_{i+1} + c_2^{i_c} s_{i+1}^2 > 0$ (over $(0,1)$) or that the derivative $N_i^{c'}$ has exactly one root $\hat{u}_{i+1} \in (0,1)$ (i.e. N_i^c has exactly one max/min/saddle at $\hat{u}_{i+1}$) and thus $N_i^c(s_{i+1}) = 0$ yields exactly single root $\hat{s}_{i+1} \in (0,1)$ - note that if $\hat{s}_{i+1} = \hat{u}_{i+1}$ then $\hat{u}_{i+1}$ is a saddle point of N_i^c. Here *a quadratic* $N_i^{c'}(s_{i+1})$ (as $\tilde{x}_{i+2} \neq \tilde{x}_i$) has coefficients $(c_0^{i_c}/6) = 5\|\tilde{x}_i\|^2 - 2\langle \tilde{x}_i | \tilde{x}_{i+2} \rangle$, $(c_1^{i_c}/6) = 5(\|\tilde{x}_{i+2}\|^2 - \|\tilde{x}_i\|^2) - 6\|\tilde{x}_{i+2} - \tilde{x}_i\|^2$, and $(c_2^{i_c}/6) = 6\|\tilde{x}_{i+2} - \tilde{x}_i\|^2 > 0$.

The discriminant $\tilde{\Delta}$ of the quadratic $N_i^{c'}(s_{i+1})/6$ reads as:

$$\tilde{\Delta} = \|\tilde{x}_{i+2}\|^4 + \|\tilde{x}_i\|^4 - 98\|\tilde{x}_{i+2}\|^2\|\tilde{x}_i\|^2 + 24\langle \tilde{x}_i | \tilde{x}_{i+2} \rangle \|\tilde{x}_{i+2} + \tilde{x}_i\|^2 \ . \tag{23}$$

Define now *two auxiliary parameters* $(\lambda, \mu) \in \Omega = (\mathbb{R}_+ \times [-1,1]) \setminus \{(1,1)\}$:

$$\|\tilde{x}_i\| = \lambda \|\tilde{x}_{i+2}\| \ , \quad \langle \tilde{x}_i | \tilde{x}_{i+2} \rangle = \mu \|\tilde{x}_i\| \|\tilde{x}_{i+2}\| \ . \tag{24}$$

ICCS Camera Ready Version 2021
To cite this paper please use the final published version:
DOI: 10.1007/978-3-030-77970-2_26

Here μ stands for $\cos(\alpha)$, where α is the angle between vectors $\tilde{x}_i$ and $\tilde{x}_{i+2}$ - hence $\mu = \lambda = 1$ is excluded as then $\tilde{x}_{i+2} = \tilde{x}_i$. Note, however that as analyzed in case *(i)* when $\tilde{x}_{i+2} = \tilde{x}_i$ there is only one optimal parameter $\hat{s}_{i+1} = 1/2$ - thus $(\mu, \lambda) = (1, 1)$ is also admissible. We examine various constraints on $(\mu, \lambda) \neq (1, 1)$ (with $\lambda > 0$ and $-1 \leq \mu \leq 1$) for the existence of either *no roots or one root* of $N_i^{c'} = 0$ over $[0, 1]$ (*yielding single critical point* of $\tilde{\mathcal{E}}_i^c$ over $(0, 1)$).

1. $\tilde{\Delta} < 0$. Since $c_2^{i_c} > 0$, clearly the following $N_i^{c'} > 0$ holds over $(0, 1)$. Substituting (24) into (23) yields (for $\Delta = (\tilde{\Delta}/\|\tilde{x}_{i+2}\|^4)$) $\Delta(\lambda, \mu) = \lambda^4 + 24\mu\lambda^3 + (48\mu^2 - 98)\lambda^2 + 24\mu\lambda + 1$. In order to decompose Ω into sub-regions Ω_- (with $\Delta < 0$), Ω_+ (with $\Delta > 0$) and Γ_0 (with $\Delta \equiv 0$) we resort to *Mathematica* functions *InequalityPlot*, *ImplicitPlot* and *Solve*. Fig. 1(a) shows the resulting decomposition and Fig. 1(b) shows its magnification for λ small. The intersection points of Γ_0 and boundary $\partial\Omega$ (found by *Solve*) read: for $\mu = 1$ it is a point $(1, 1)$ (already excluded - see dotted point in Fig. 1) and for $\mu = -1$ we have two points $(-1, (1/(13 + 2\sqrt{42}))) \approx (-1, 0.0385186)$ or $(-1, 13 + 2\sqrt{42}) \approx (-1, 25.9615)$.

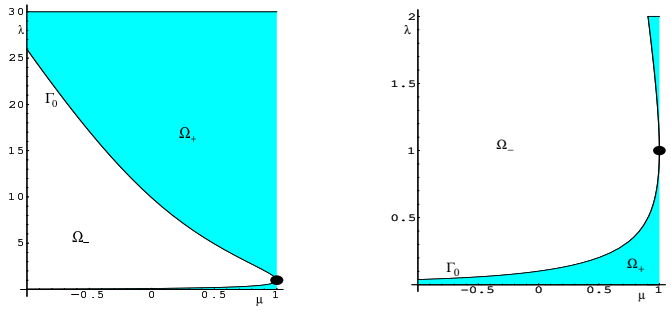

(a) (b)

Fig. 1. Decomposition of Ω into sub-regions: (a) over which $\Delta > 0$ (i.e. Ω_+), $\Delta = 0$ (i.e. Γ_0) or $\Delta < 0$ (i.e. Ω_-), (b) only for λ small.

The admissible subset $\Omega_{ok} \subset \Omega$ of parameters (μ, λ) (*for which there is one local minimum of* $\tilde{\mathcal{E}}_i^c$) satisfies $\Omega_- \subset \Omega_{ok}$. The set to $\Omega \setminus \Omega_-$ is a potential *exclusion zone* $\Omega_{ex} \subset \Omega \setminus \Omega_-$. Next we shrink an exclusion zone $\Omega_{ex} \subset \Omega$ (subset of shaded region in Fig. 1).

2. $\tilde{\Delta} = 0$. There is only one root $\hat{u}_{i+1}^0 \in \mathbb{R}$ for $N_i^{c'}(s_{i+1}) = 0$. As explained, irrespectively whether $\hat{u}_{i+1}^0 \in (0, 1)$ or $\hat{u}_{i+1}^0 \notin (0, 1)$ this results in exactly one root $\hat{s}_{i+1} \in (0, 1)$ of $N_i^c(s_{i+1}) = 0$, which in turn yields exactly one local (thus one global) minimum for $\tilde{\mathcal{E}}_i^c$. Hence $\Omega_- \cup \Gamma_0 \subset \Omega_{ok}$.

3. $\tilde{\Delta} > 0$. There are two different roots $\hat{u}_{i+1}^{\pm} \in \mathbb{R}$ of $N_i^{c'}(s_{i+1}) = 0$. Note that since $c_2^{i_c} > 0$ we have $\hat{u}_{i+1}^- < \hat{u}_{i+1}^+$. They are either (in all cases we use Vieta's formulas):

(a) of *opposite signs*: i.e. $(c_0^{i_c}/c_2^{i_c}) < 0$ or

(b) non-positive: i.e. $(c_0^{i_c}/c_2^{i_c}) \geq 0$ and $(-c_1^{i_c}/c_2^{i_c}) < 0$ (as $\hat{u}_{i+1}^- < \hat{u}_{i+1}^+$) or

ICCS Camera Ready Version 2021
To cite this paper please use the final published version:
DOI: 10.1007/978-3-030-77970-2_26

(c) non-negative: i.e. $(c_0^{i_c}/c_2^{i_c}) \geq 0$ and $(-c_1^{i_c}/c_2^{i_c}) > 0$ - split into:
(c1) $\hat{u}_{i+1}^{+} \geq 1$: i.e.
(c2) $0 < \hat{u}_{i+1}^{+} < 1$ (as here $\hat{u}_{i+1}^{-} < \hat{u}_{i+1}^{+}$).

Evidently for a), b) and c1) there is *up to one root* $\hat{u}_{i+1} \in (0,1)$ of $N_i^{c'}(s_{i+1}) = 0$. Therefore as already explained there is only one root $\hat{s}_{i+1} \in (0,1)$ of $N_i^{c}(s_{i+1}) = 0$, which is the unique critical point of $\tilde{\mathcal{E}}_i^c$ over $(0,1)$. We show now that the inequalities from a) or b) or c) extend (contract) the admissible (exclusion) zone Ω_{ok} (Ω_{ex}) of parameters $(\mu,\lambda) \in \Omega$. Indeed:

a) the constraint $(c_0^{i_c}/c_2^{i_c}) < 0$ upon using (24) reads (as $\lambda > 0$):

$$5\lambda^2 - 2\mu\lambda < 0 \quad \equiv \lambda < \frac{2\mu}{5}\,. \tag{25}$$

Fig. 2 a) shows Ω_1 (over which (25) holds) cut out from the exclusion zone Ω_{ex} of parameters $(\mu,\lambda) \in \Omega$ (again *InequalityPlot* is used here).

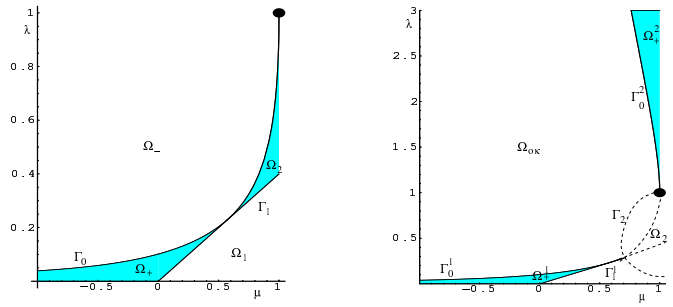

(a) (b)

Fig. 2. Extension of admissible zone Ω_{ok} by cutting out from Ω_{ex}: (a) Ω_1, (b) Ω_2.

Thus $\Omega_- \cup \Gamma_0 \cup \Omega_1 \subset \Omega_{ok}$. The intersection $\Gamma_1 \cap \partial\Omega = \{(0,0),(1,0.4)\}$ (here $\Gamma_1 = \{(\mu,\lambda) \in \Omega : 5\lambda - 2\mu = 0\}$). Similarly the intersection $\Gamma_0 \cap \Gamma_1 = \{(5/(2\sqrt{19}), 1/\sqrt{19})\} \approx (0.573539, 0.229416) = p_1$.

b) the constraints $(c_0^{i_c}/c_2^{i_c}) \geq 0$ and $(-c_1^{i_c}/c_2^{i_c}) < 0$ combined with (24) yield:

$$\lambda \geq \frac{2\mu}{5} \quad \text{and} \quad 11\lambda^2 - 12\mu\lambda + 1 < 0\,. \tag{26}$$

Using *ImplicitPlot* and *InequalityPlot* we find Ω_2 (cut out from Ω_{ex}) as the intersection of three sets defined by (26) and $\Delta > 0$ (for Ω_2 see Fig. 2 a-b)). Thus $\Omega_- \cup \Gamma_0 \cup \Omega_1 \cup \Omega_2 \subset \Omega_{ok}$ (see Fig. 2 b)). Note that for $\Gamma_2 = \{(\mu,\lambda) \in \Omega : 11\lambda^2 - 12\mu\lambda + 1 = 0\}$ the sets $\Gamma_0 \cap \Gamma_2 = \{(5/(2\sqrt{19}), 1/\sqrt{19}), (1,1)\}$, $\Gamma_1 \cap \Gamma_2 = \{(5/(2\sqrt{19}), 1/\sqrt{19})\}\}$, and intersection of Γ_2 with the boundary $\mu = 1$ yields $\{(1,1),(1,1/11)\}\}$ (use e.g. *Solve* in *Mathematica*).

c1) $(c_0^{i_c}/c_2^{i_c}) \geq 0$, $(-c_1^{i_c}/c_2^{i_c}) > 0$ and $u_{i+1}^{+} \geq 1$ with (24) yield

$$\lambda \geq \frac{2\mu}{5}\,, \quad 11\lambda^2 - 12\mu\lambda + 1 > 0\,, \quad \sqrt{\Delta} \geq \lambda^2 - 12\mu\lambda + 11\,. \tag{27}$$

ICCS Camera Ready Version 2021
To cite this paper please use the final published version:
DOI: 10.1007/978-3-030-77970-2_26

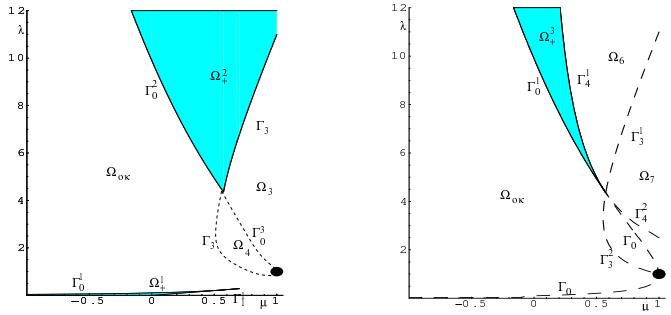

Fig. 3. Extension of admissible zone Ω_{ok} by cutting out from Ω_{ex}: (a) Ω_3, (b) Ω_4.

The last inequality in (27) is clearly satisfied for $\lambda^2 - 12\mu\lambda + 11 < 0$. This holds over $\Omega_5 = \Omega_3 \cup \Omega_4 \cup \Gamma_0^3$ which is the domain bounded by $\Gamma_3 = \{(\mu, \lambda) \in \Omega : \lambda^2 - 12\mu\lambda + 11 = 0\}$ and the boundary $\mu = 1$ (see Fig. 3 a)). Here $\Gamma_3 \cap \partial\Omega = \{(1,1),(1,11)\}$ and $\Gamma_3 \cap \Gamma_0 = \{(1,1),(5/(2\sqrt{19}),\sqrt{19})\} \approx \{(1,1),(0.573539,4.3589)\}$ - again we resort here to *InequalityPlot*, *ImplicitPlot* and *Solve* functions in *Mathematica*. Intersecting Ω_5 with three subsets defined by the first two inequalities from (27) and $\Delta > 0$ yields cutting Ω_3 from the exclusion zone Ω_{ex} (see Fig. 3 a)), where Ω_3 is bounded by Γ_0^3, undashed Γ_3 and the boundary $\mu = 1$. Thus $\Omega_- \cup \Gamma_0 \cup \Omega_1 \cup \Omega_2 \cup \Omega_3 \subset \Omega_{ok}$. For the opposite case $\lambda^2 - 12\mu\lambda + 11 \geq 0$ (satisfied over $\Omega \setminus \Omega_5$) the last inequality from (27) yields $\Omega_8 = \Omega_6 \cup \Omega_7 \cup \Gamma_3^1$ with the bounding curve $\Gamma_4 = \{(\mu, \lambda) \in \Omega : \Delta - (\lambda^2 - 12\mu\lambda + 11)^2 = 0\}$ (see Fig. 3 b)) - here Ω_6 is bounded by Γ_4^1, Γ_3^1 and $\partial\Omega$ and Ω_7 is bounded by Γ_4^2, Γ_3^1 and $\partial\Omega$). The intersection of Γ_4 with boundary $\mu = 1$ yields single point $\{(1, 5/2)\}$. Since $\Gamma_0 \cap \Gamma_3 \cap \Gamma_4 = \{(5/(2\sqrt{19}),\sqrt{19})\} \approx \{(0.573539,4.3589)\} = p_2$ the intersection of Ω_8 with the regions defined by first two inequalities in (27) (and by $\Delta > 0$ and $\lambda^2 - 12\mu\lambda + 11 \geq 0$) leads to the further cut out of $\Omega_6 \cup \Gamma_4^1 \cup \Gamma_3^1$ in the zone $\Omega_+^3 \subset \Omega_{ex}$. The inclusion $\Omega_- \cup \Gamma_0 \cup \Omega_1 \cup \Omega_2 \cup \Omega_3 \cup \Omega_6 \cup \Gamma_4^1 \cup \Gamma_3^1 \subset \Omega_{ok}$ follows.

5 Perturbed Special Case

Assume now that for data points $\{\tilde{x}_i, \tilde{x}_{i+1}, \tilde{x}_{i+2}\}$ and velocities $\{\tilde{v}_i, \tilde{v}_{i+2}\}$ condition (20) is not met. For the *perturbation vector* $\delta = (\delta_1, \delta_2) \in \mathbb{R}^{2m}$ we attempt to extend the results for (20) to its perturbed form (28). Indeed let (δ_1, δ_2):

$$\tilde{x}_{i+2} - \tilde{x}_i - \tilde{v}_{i+2} = \delta_1 \ , \qquad \tilde{v}_{i+2} - \tilde{v}_i = \delta_2 \ , \tag{28}$$

with $\tilde{\mathcal{E}}_i^{\delta}$ derived as in (18). Of course, for $\delta_1 = \delta_2 = \mathbf{0} \in \mathbb{R}^m$ (28) collapses to (20) (i.e. with the notation $\tilde{\mathcal{E}}_i^0 = \bar{\mathcal{E}}_i^c$ derived for (20)). To obtain formulas for $\tilde{\mathcal{E}}_i^{\delta}$

ICCS Camera Ready Version 2021
To cite this paper please use the final published version:
DOI: 10.1007/978-3-030-77970-2_26

and $\tilde{\mathcal{E}}_i^{\delta'}$ we resort to (by (28)):

$$\begin{aligned}
\|\tilde{v}_{i+2}\|^2 &= \|\tilde{x}_{i+2}\|^2 + \|\tilde{x}_i\|^2 - 2\langle\tilde{x}_i|\tilde{x}_{i+2}\rangle - 2\langle\tilde{x}_{i+2}|\delta_1\rangle + 2\langle\tilde{x}_i|\delta_1\rangle + \|\delta_1\|^2 \ , \\
\langle\tilde{v}_{i+2}|\tilde{x}_i\rangle &= \langle\tilde{x}_i|\tilde{x}_{i+2}\rangle - \|\tilde{x}_i\|^2 - \langle\tilde{x}_i|\delta_1\rangle \ , \\
\langle\tilde{v}_{i+2}|\tilde{x}_{i+2}\rangle &= \|\tilde{x}_{i+2}\|^2 - \langle\tilde{x}_i|\tilde{x}_{i+2}\rangle - \langle\tilde{x}_{i+2}|\delta_1\rangle \ , \\
\|\tilde{v}_i\|^2 &= \|\tilde{x}_{i+2}\|^2 + \|\tilde{x}_i\|^2 - 2\langle\tilde{x}_i|\tilde{x}_{i+2}\rangle + \|\delta_1\|^2 + \|\delta_2\|^2 + 2\langle\delta_1|\delta_2\rangle \\
&\quad -2\langle\tilde{x}_{i+2}|\delta_1\rangle - 2\langle\tilde{x}_{i+2}|\delta_2\rangle + 2\langle\tilde{x}_i|\delta_1\rangle + 2\langle\tilde{x}_i|\delta_2\rangle \ , \\
\langle\tilde{v}_i|\tilde{v}_{i+2}\rangle &= \|\tilde{x}_{i+2}\|^2 + \|\tilde{x}_i\|^2 - 2\langle\tilde{x}_i|\tilde{x}_{i+2}\rangle - 2\langle\tilde{x}_{i+2}|\delta_1\rangle + 2\langle\tilde{x}_i|\delta_1\rangle - \langle\tilde{x}_{i+2}|\delta_2\rangle \\
&\quad +\langle\tilde{x}_i|\delta_2\rangle + \|\delta_1\|^2 + \langle\delta_1|\delta_2\rangle \ , \\
\langle\tilde{x}_i|\tilde{v}_i\rangle &= \langle\tilde{x}_i|\tilde{x}_{i+2}\rangle - \|\tilde{x}_i\|^2 - \langle\tilde{x}_i|\delta_1\rangle - \langle\tilde{x}_i|\delta_2\rangle \ , \\
\langle\tilde{x}_{i+2}|\tilde{v}_i\rangle &= \|\tilde{x}_{i+2}\|^2 - \langle\tilde{x}_i|\tilde{x}_{i+2}\rangle - \langle\tilde{x}_{i+2}|\delta_1\rangle - \langle\tilde{x}_{i+2}|\delta_2\rangle \ ,
\end{aligned}$$

leading by (18) to (with *FullSimplify*, *Factor* and *CoefficientList*): $\tilde{\mathcal{E}}_i^{\delta}(s_{i+1}) =$

$$\begin{aligned}
&\frac{1}{s_{i+1}^3(s_{i+1}-1)^3}(3\|\tilde{x}_i\|^2(s_{i+1}-1)^3(1+3s_{i+1}) + s_{i+1}(-6(\langle\tilde{x}_i|\tilde{x}_{i+2}\rangle \\
&-\langle\tilde{x}_i|\delta_1\rangle - \langle\tilde{x}_i|\delta_2\rangle - \|\tilde{x}_i\|^2) + s_{i+1}(-18\langle\tilde{x}_i|\tilde{x}_{i+2}\rangle(s_{i+1}-1)^2 \\
&-6(\langle\tilde{x}_i|\tilde{x}_{i+2}\rangle - \langle\tilde{x}_i|\delta_1\rangle - \|\tilde{x}_i\|^2)(s_{i+1}-1)^3 + 6(-\langle\tilde{x}_i|\tilde{x}_{i+2}\rangle - \langle\tilde{x}_{i+2}|\delta_1\rangle \\
&+\|\tilde{x}_{i+2}\|^2)(s_{i+1}-2)(s_{i+1}-1)s_{i+1} - 6(-\langle\tilde{x}_i|\tilde{x}_{i+2}\rangle - \langle\tilde{x}_{i+2}|\delta_1\rangle \\
&-\langle\tilde{x}_{i+2}|\delta_2\rangle + \|\tilde{x}_{i+2}\|^2)(s_{+1}-1)^2 s_{i+1} + (-2\langle\tilde{x}_i|\tilde{x}_{i+2}\rangle + 2\langle\tilde{x}_i|\delta_1\rangle \\
&-2\langle\tilde{x}_{i+2}|\delta_1\rangle + \|\tilde{x}_i\|^2 + \|\tilde{x}_{i+2}\|^2 + \|\delta_1\|^2)(s_{i+1}-4)(s_{i+1}-1)^2 s_{i+1} \\
&-2(-2\langle\tilde{x}_i|\tilde{x}_{i+2}\rangle + 2\langle\tilde{x}_i|\delta_1\rangle + \langle\tilde{x}_i|\delta_2\rangle - 2\langle x_{i+2}|\delta_1\rangle - \langle\tilde{x}_{i+2}|\delta_1\rangle + \langle\delta_1|\delta_2\rangle \\
&+\|\tilde{x}_i\|^2 + \|\tilde{x}_{i+2}\|^2 + \|\delta_1\|^2)(s_{i+1}-1)^3 s_{i+1} + (-2\langle\tilde{x}_i|\tilde{x}_{i+2}\rangle + 2\langle\tilde{x}_i|\delta_1\rangle \\
&+2\langle\tilde{x}_i|\delta_2\rangle - 2\langle\tilde{x}_{i+2}|\delta_1\rangle - 2\langle\tilde{x}_{i+2}|\delta_2\rangle + 2\langle\delta_1|\delta_2\rangle + \|\tilde{x}_i\|^2 + \|\tilde{x}_{i+2}\|^2 + \|\delta_1\|^2 \\
&+\|\delta_2\|^2)(s_{i+1}-1)^3(3+s_{i+1}) + 3\|\tilde{x}_{i+2}\|^2 s_{i+1}(3s_{i+1}-4) \\
&+6(\langle\tilde{x}_i|\tilde{x}_{i+2}\rangle - \langle\tilde{x}_i|\delta_1\rangle - \langle\tilde{x}_i|\delta_2\rangle - \|\tilde{x}_i\|^2)(2+(s_{i+1}-2)s_{i+1}^2))))
\end{aligned} \tag{29}$$

yielding $\tilde{\mathcal{E}}_i^{\delta}(s_{i+1}) = M_i^{\delta}(s_{i+1})/(s_{i+1}^3(s_{i+1}-1)^3)$. Here $deg(M_i^{\delta}) = 6$ with the coefficients (using *Mathematica* functions *Factor* and *CoefficientList*): $a_0^{i,\delta} = -3\|\tilde{x}_i\|^2$, $a_1^{i,\delta} = -6\langle\tilde{x}_i|\tilde{x}_{i+2}\rangle + 6\langle\tilde{x}_i|\delta_1\rangle + 6\langle\tilde{x}_i|\delta_2\rangle + 6\|\tilde{x}_i\|^2$, $a_2^{i,\delta} = 6\langle\tilde{x}_i|\tilde{x}_{i+2}\rangle - 24\langle\tilde{x}_i|\delta_1\rangle - 18\langle\tilde{x}_i|\delta_2\rangle + 6\langle\tilde{x}_{i+2}|\delta_1\rangle + 6\langle\tilde{x}_{i+2}|\delta_2\rangle - 6\langle\delta_1|\delta_2\rangle - 3\|\tilde{x}_i\|^2 - 3\|\tilde{x}_{i+2}\|^2 - 3\|\delta_1\|^2 - 3\|\delta_2\|^2$, $a_3^{i,\delta} = 2(15\langle\tilde{x}_i|\delta_1\rangle + 9\langle\tilde{x}_i|\delta_2\rangle - 9\langle\tilde{x}_{i+2}|\delta_1\rangle - 6\langle\tilde{x}_{i+2}|\delta_2\rangle + 9\langle\delta_1|\delta_2\rangle + 3\|\delta_1\|^2 + 4\|\delta_2\|^2)$, $a_4^{i,\delta} = -12\langle\tilde{x}_i|\delta_1\rangle - 6\langle\tilde{x}_i|\delta_2\rangle + 12\langle\tilde{x}_{i+2}|\delta_1\rangle + 6\langle\tilde{x}_{i+2}|\delta_2\rangle - 18\langle\delta_1|\delta_2\rangle - 3\|\delta_1\|^2 - 6\|\delta_2\|^2$, $a_5^{i,\delta} = 6\langle\delta_1|\delta_2\rangle$ and $a_6^{i,\delta} = \|\delta_2\|^2$. The derivative of $\tilde{\mathcal{E}}_i^{\delta}(s_{i+1})$ reads as $\tilde{\mathcal{E}}_i^{\delta'}(s_{i+1}) = -N_i^{\delta}(s_{i+1})/(s_{i+1}^4(s_{i+1}-1)^4)$, where N_i^{δ} is the 6-th order polynomial in s_{i+1} with the coefficients (e.g. again upon using symbolic differentiation in *Mathematica* and functions *Factor* and *CoefficientList*): $b_0^{i,\delta} = -9\|\tilde{x}_i\|^2$, $b_1^{i,\delta} = -12\langle\tilde{x}_i|\tilde{x}_{i+2}\rangle + 12\langle\tilde{x}_i|\delta_1\rangle + 12\langle\tilde{x}_i|\delta_2\rangle + 30\|\tilde{x}_i\|^2$, $b_2^{i,\delta} = 3(12\langle\tilde{x}_i|\tilde{x}_{i+2}\rangle - 18\langle\tilde{x}_i|\delta_1\rangle - 16\langle\tilde{x}_i|\delta_2\rangle + 2\langle\tilde{x}_{i+2}|\delta_1\rangle + 2\langle\tilde{x}_{i+2}|\delta_2\rangle - 2\langle\delta_1|\delta_2\rangle - 11\|\tilde{x}_i\|^2 - \|\tilde{x}_{i+2}\|^2 - \|\delta_1\|^2 - \|\delta_2\|^2)$, $b_3^{i,\delta} = 3(-8\langle\tilde{x}_i|\tilde{x}_{i+2}\rangle + 32\langle\tilde{x}_i|\delta_1\rangle + 24\langle\tilde{x}_i|\delta_2\rangle - 8\langle\tilde{x}_{i+2}|\delta_1\rangle - 8\langle\tilde{x}_{i+2}|\delta_2\rangle + 8\langle\delta_1|\delta_2\rangle + 4\|\tilde{x}_i\|^2 + 4\|\tilde{x}_{i+2}\|^2 + 4\|\delta_1\|^2 + 4\|\delta_2\|^2)$, $b_4^{i,\delta} =$

ICCS Camera Ready Version 2021
To cite this paper please use the final published version:
DOI: 10.1007/978-3-030-77970-2_26

$3(-26\langle\tilde{x}_i|\delta_1\rangle-16\langle\tilde{x}_i|\delta_2\rangle+14\langle\tilde{x}_{i+2}|\delta_1\rangle+10\langle\tilde{x}_{i+2}|\delta_2\rangle-12\langle\delta_1|\delta_2\rangle-5\|\delta_1\|^2-6\|\delta_2\|^2)$, $b_5^{i,\delta}=3(8\langle\tilde{x}_i|\delta_1\rangle+4\langle\tilde{x}_i|\delta_2\rangle-8\langle\tilde{x}_{i+2}|\delta_1\rangle-4\langle\tilde{x}_{i+2}|\delta_2\rangle+8\langle\tilde{\delta}_1|\delta_2\rangle+2\|\delta_1\|^2+4\|\delta_2\|^2)$ and $b_6^{i,\delta}=-6\langle\delta_1|\delta_2\rangle-3\|\delta_2\|^2$.

The following result merging (20) with (28) holds (proof is omitted):

Theorem 1. *Assume that for unperturbed data* (20) *the corresponding energy* $\tilde{\mathcal{E}}_i^0$ *has exactly one critical point* $\hat{s}_0\in(0,1)$ *with* $\tilde{\mathcal{E}}_i^{0''}(\hat{s}_0)\neq 0$. *Then there exists sufficiently small* $\varepsilon_0>0$ *such that for all* $\|\delta\|<\varepsilon_0$ *(where* $\delta=(\delta_1,\delta_2)\in\mathbb{R}^{2m}$*) the perturbed data* (28) *yield the energy* $\tilde{\mathcal{E}}_i^\delta$ *with exactly one critical point* $\hat{s}_0^\delta\in(0,1)$ *(a global minimum* $\hat{s}_0^\delta$ *of* $\tilde{\mathcal{E}}_i^\delta$ *is sufficiently close to* $\hat{s}_0$*).*

Example 1. Consider the planar points $\tilde{x}_i=(0,-1)$, $\tilde{x}_{i+1}=(0,0)$ and $\tilde{x}_{i+2}=(1,1)$ - we set here $i=0$. Here cumulative chord parameterization yields $\hat{s}_1^{cc}=1/(\sqrt{2}+1)\approx 0.414214$. Assume that given velocities $\tilde{v}_0,\tilde{v}_2$ (upon adjustment by some perturbation $\delta=(\bar{\delta},\hat{\delta})\in\mathbb{R}^4$) satisfy both constraints $\tilde{x}_2-\tilde{x}_0=\tilde{v}_2+\bar{\delta}$ and $\tilde{v}_2=\tilde{v}_0+\hat{\delta}$. The above interpolation points $\{\tilde{x}_i,\tilde{x}_{i+1},\tilde{x}_{i+2}\}$ for further testing in this example are assumed to be fixed. Here $\|\tilde{x}_0\|^2=1$, $\|\tilde{x}_2\|^2=2$, $\langle\tilde{x}_0|\tilde{x}_2\rangle=-1$ and $(\mu,\lambda)=(-1/\sqrt{2},1/\sqrt{2})\approx(-0.707107,0.707107)\in\Omega_{ok}$ (with $\delta=\mathbf{0}$). The unperturbed energy with $\tilde{v}_2=\tilde{v}_0=(1,2)$ (see also (21) or (29) with $\delta=\mathbf{0}$ and non-perturbed data satisfying (20)) amounts to: $\tilde{\mathcal{E}}_0^\delta(s)=-3(1+s(5s-4))((s-1)^3s^3)^{-1}$. which yields a global minimum $\tilde{\mathcal{E}}_0^c(0.433436)=41.6487$ (see Fig. 4). As here $(\mu,\lambda)=(-1/\sqrt{2},1/\sqrt{2})\in\Omega_{ok}$ and thus $\tilde{\mathcal{E}}_0^0$ has exactly one critical point $\hat{s}_0\in(0,1)$. One can show that $\tilde{\mathcal{E}}_0^{0''}\neq 0$ at any critical point $\hat{s}_0$ of $\tilde{\mathcal{E}}_0^0$. Hence the assumptions from Th. 1 are clearly satisfied.

We add now the perturbation $\bar{\delta}=(2,-3)$ and $\hat{\delta}=(-1,2)$ (for $\tilde{v}_0=(0,3)$ and $\tilde{v}_2=(-1,5)$). The corresponding perturbed energy (see (29)) $\tilde{\mathcal{E}}_0^\delta(s)=(-3+s(18+s(-57+s(34+s(45+s(5s-48))))))((s-1)^3s^3)^{-1}$ is plotted in Fig. 5 with the optimal value $\hat{s}_0^\delta\approx 0.390407$ (close to $\hat{s}_1^{cc}$ as perturbation δ is sufficiently small - here $(\|\bar{\delta}\|,\|\hat{\delta}\|)=(\sqrt{13},\sqrt{5})$) and $\tilde{\mathcal{E}}_\delta^c(\hat{s}_0^\delta)=149.082<\tilde{\mathcal{E}}_\delta^c(\hat{s}_1^{cc})=150.004$ - the convexity of $\tilde{\mathcal{E}}_0^c$ is visibly preserved by $\tilde{\mathcal{E}}_\delta^c$ (see Fig. 4 and Fig. 5).

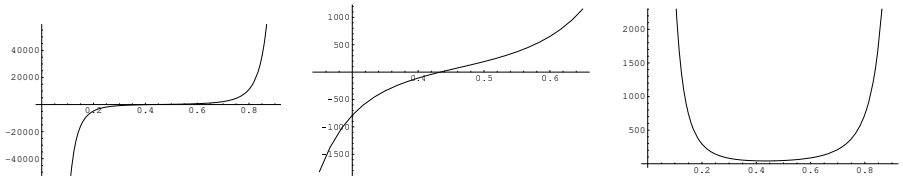

(a) (b) (c)

Fig. 4. The graph of $\tilde{\mathcal{E}}_0^{c'}$ for $\tilde{x}_0=(0,-1)$, $\tilde{x}_2=(1,1)$, $\tilde{v}_0=\tilde{v}_2=(1,2)$ (a) over $(0,1)$, (b) close to unique root $\hat{s}_0\approx 0.433\neq\hat{s}_1^{cc}=1/(\sqrt{2}+1)\approx 0.414$, (c) the graph of $\tilde{\mathcal{E}}_0^c$.

For a large perturbation $\bar{\delta}=(16,7)$ and $\hat{\delta}=(-10,5)$ (for $\tilde{v}_0=(-5,-10)$ and $\tilde{v}_2=(-15,-5)$) the corresponding perturbed energy (see (29) and use *Simplify* in *Mathematica*) $\tilde{\mathcal{E}}_0^\delta(s)=(-3+s(-60+s(-189+s(-74+5s(5s-$

ICCS Camera Ready Version 2021
To cite this paper please use the final published version:
DOI: 10.1007/978-3-030-77970-2_26

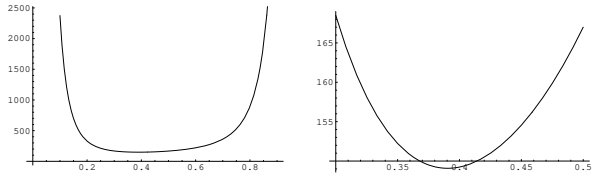

(a) (b)

Fig. 5. The graph of $\tilde{\mathcal{E}}^c_\delta$ for $\tilde{x}_0 = (0,-1)$, $\tilde{x}_2 = (1,1)$, $\tilde{v}_0 = (0,3)$, $\tilde{v}_2 = (-1,5)$, $\bar{\delta} = (2,-3)$ and $\hat{\delta} = (-1,2)$ (a) over $(0,1)$, (b) close to its unique min. $\hat{s}^\delta_0 = 0.390 \neq s^{cc}_1 = 1/(\sqrt{2}+1) \approx 0.414$.

$21)(5s-9)))))((s-1)^3 s^3)^{-1}$ is plotted in Fig. 6 a) with the unique optimal value $\hat{s}^\delta_0 \approx 0.432069$ for which $\tilde{\mathcal{E}}^c_\delta(\hat{s}^\delta_0) = 3229.81 < \tilde{\mathcal{E}}^c_\delta(\hat{s}^{cc}_1) = 3236.5$ - the convexity of $\tilde{\mathcal{E}}^c_0$ is here visibly also preserved by $\tilde{\mathcal{E}}^c_\delta$ (even for such a quite large perturbation δ - here $(\|\bar{\delta}, \|\hat{\delta}\|) = (125, 305)$). Note also that though cumulative chord $\hat{s}^{cc}_1$ is now farther away from a global minimum $\hat{s}^\delta_0$, it is still in its potential basin.

We add now very large $\bar{\delta} = (-25,-17)$ and $\hat{\delta} = (-6,20)$ (for $\tilde{v}_0 = (32,-1)$ and $\tilde{v}_2 = (26,19)$). The perturbed energy (see (29)) $\tilde{\mathcal{E}}^\delta_0(s) = (-3 + s(-6 + s(-3141 + 2s(3145 + s(-1221 - 570s + 218s^2)))))((s-1)^3 s^3)^{-1}$ is plotted in Fig. 6 b) with the optimal value $\hat{s}^\delta_0 \approx 0.948503$ for which $\tilde{\mathcal{E}}^c_\delta(\hat{s}^\delta_0) = 11146 < \tilde{\mathcal{E}}^c_\delta(\hat{s}^{cc}_1) = 12667.7$ and another local minimum at $\hat{s}^1_0 \approx 0.563968$ for which $\tilde{\mathcal{E}}^c_\delta(\hat{s}^1_0) = 11781$. There is also a local maximum at $\hat{s}_{max} \approx 0.879929 > s^{cc}_1 = 1/3$ - convexity of $\tilde{\mathcal{E}}^c_0$ is here clearly not preserved by $\tilde{\mathcal{E}}^c_\delta$ (δ is here too large for Th. 1 to hold - here $(\|\bar{\delta}\|, \|\hat{\delta}\|) = (914, 436)$) - see also Fig. 4 and Fig. 6. Again the cumulative chord $\hat{s}^{cc}_1 \approx 0.414214$ is here in the basin of $\hat{s}^1_0$ (not of $\hat{s}^\delta_0$) - see Fig. 6 b). □

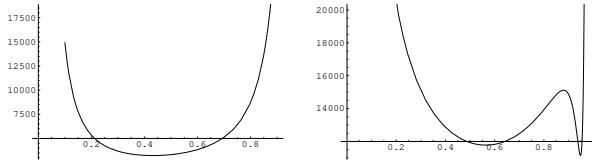

(a) (b)

Fig. 6. The graph of $\tilde{\mathcal{E}}^c_\delta$ for $\tilde{x}_0 = (0,-1)$ and $\tilde{x}_2 = (1,1)$ for (a) $\tilde{v}_0 = (-5,-10)$, $\tilde{v}_2 = (-15,-5)$ and a big $\bar{\delta} = (-16,7)$ and $\bar{\delta} = (-10,5)$ yielding global min. at $\hat{s}^\delta_0 \approx 0.432 \neq s^{cc}_1 \approx 0.414$, (b) $\tilde{v}_0 = (32,-1)$, $\tilde{v}_2 = (26,19)$ and a very big $\bar{\delta} = (-25,-17)$ and $\bar{\delta} = (-6,20)$ with global min. at $\hat{s}^\delta_0 \approx 0.949$ and a local min. at $\hat{s}^1_0 = 0.564 \neq s^{cc}_1 \approx 0.414$.

Ex. 1 hints that δ in Th. 1 can in fact be quite substantial. Thus a local character of Th. 1 seems to be more a semi-global one.

ICCS Camera Ready Version 2021
To cite this paper please use the final published version:
DOI: 10.1007/978-3-030-77970-2_26

6 Conclusions

This work discusses the problem of finding the optimal knots to fit reduced data. The optimization task (1) is reformulated into (5) (and (18)) to minimize a highly non-linear multivariable function $\mathcal{J}_0$ depending on knots $\mathcal{T}_{int}$. A feasible numerical scheme to handle (5) is *a Leap-Frog*. It minimizes iteratively single variable functions from (6). Generic case of *Leap-Frog* is addressed to establish sufficient conditions for unimodality of (18). First, its special case (20) is studied. Next a perturbed analogue (28) of the latter is addressed. The unimodality of (21) is shown to be preserved by large perturbations (28). The performance of *Leap-Frog* in minimizing (5) against *Newton's* and *Secant Methods* is discussed in [2], [3] and [6]. Other contexts and applications of *Leap-Frog* can be found in [9], [10] or [11]. For more work on fitting $\mathcal{M}_n$ (sparse or dense) see [4], [5] or [7].

References

1. de Boor, C.: A Practical Guide to Splines. 2nd edn. Springer-Verlag, New York (2001). https://www.springer.com/gp/book/9780387953663
2. Kozera, R., Noakes L.: Optimal knots selection for sparse reduced data. In: Huang, F., Sugimoto, A. (eds.) PSIVT 2015, pp. 3–14. LNCS Vol. 9555, Springer Int. Pub. (2016). https://doi.org/10.1007/978-3-319-30285-0_1
3. Kozera, R., Noakes L.: Non-linearity and non-convexity in optimal knots selection for sparse reduced data. In: Gerdt, V.P., et al. (eds.) CASC 2017, pp. 257–271. LNCS vol. 10490, Springer Int. Pub. (2017). https://doi.org/10.1007/978-3-319-66320-3_19
4. Kozera, R., Noakes L., Wilkołazka, M.: Parameterizations and Lagrange cubics for fitting multidimesional data. In: Krzhizhanovskaya, V.V., et al. (eds.) ICCS 2020, pp. 124–140. LNCS vol. 12138, Springer Cham (2020). https://doi.org/10.1007/978-3-030-50417-5_10
5. Kozera, R., Noakes L., Wilkołazka, M.: Exponential parameterization to fit reduced data. J. Comput. Appl. Math. **391**(C), 125645 (2021). https://doi.org/10.1016/j.amc.2020.125645
6. Kozera, R., Wiliński A.: Fitting dense and sparse reduced data. In: Pejaś, J. et al. (eds.) ACS 2018, pp. 3–17. In: Advances in Intelligent Systems and Computing vol. 889, Springer Nature Switzerland AG (2019). https://doi.org/10.1007/978-3-030-03314-9_1
7. Kuznetsov, E.B., Yakimovich A.Y.: The best parameterization for parametric interpolation. Appl. Math. Comput. **191**(2), 239–245 (2006). https://core.ac.uk/download/pdf/81959885.pdf
8. Kvasov, B.I.: Methods of Shape-Preserving Spline Approximation. World Scientific Pub., Singapore (2000). https://doi.org/10.1142/4172
9. Matebese, B., Withey, D., Banda M.K.: Modified Newton's method in the Leapfrog method for mobile robot path planning. In: Dash, S.S., et al. (eds.) ICAIECES 2017, pp. 71–78. Advances in Intelligent Systems and Computing vol. 668, Springer Nature Singapore (2018). https://doi.org/10.1007/978-981-10-7868-2_7
10. Noakes, L.: A global algorithm for geodesics. J. Aust. Math. Soc. Series A **65**(1), 37–50 (1998). https://doi.org/10.1017/S1446788700039380
11. Noakes, L., Kozera, R.: Nonlinearities and noise reduction in 3-source photometric stereo. J. Math. Imaging Vision **18**(2), 119–127 (2003). https://doi.org/10.1023/A:1022104332058

ICCS Camera Ready Version 2021
To cite this paper please use the final published version:
DOI: 10.1007/978-3-030-77970-2_26